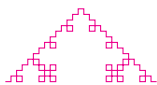




DØ Detector

Sina Bahrasemani



November 27, 2017

Outline



DØ experiment

Central tracking

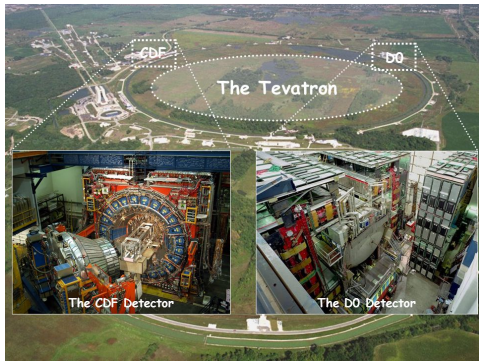
Preshower detectors

Calorimeter

Muon system

Trigger System

D \emptyset Experiment



Aerial view of Fermilab National Accelerator Laboratory

- probed $\sqrt{s} = 1.96\text{TeV}$ $p - \bar{p}$ collisions at a rate of $1.2 \times 10^6 \text{s}^{-1}$ ($\approx \mathcal{L}_{int} = 10 \text{fb}^{-1}$)

DØ Experiment Goals



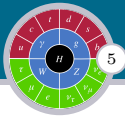
□ Precision searches:

- ▶ Z and W masses, widths and production cross sections
- ▶ Forward-backward asymmetry
- ▶ $W/Z \rightarrow q\bar{q}$
- ▶ $\frac{\alpha_{QCD}}{\alpha_{QED}}$
- ▶ Gauge boson couplings

□ New physics:

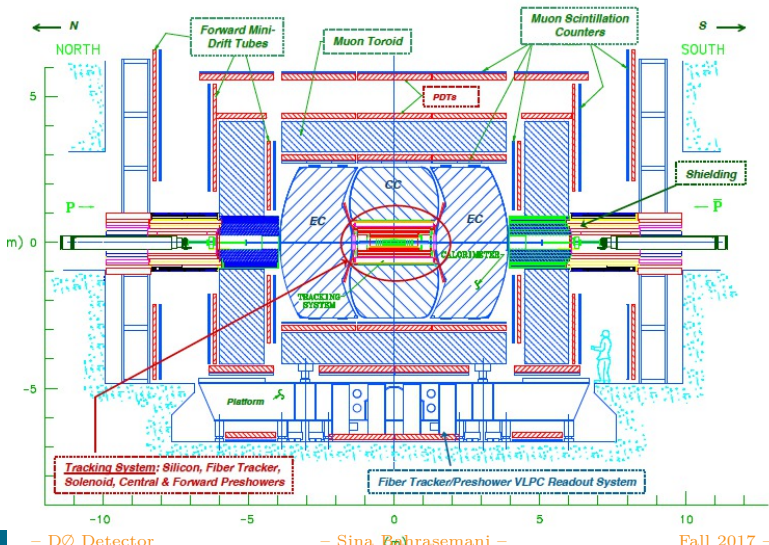
- ▶ $Z \rightarrow X\gamma; X \rightarrow l^+l^-$
- ▶ top
- ▶ Higgs boson
- ▶ Supersymmetry
- ▶ W', Z' , heavy leptons and heavy quarks
- ▶ Surprises !

DØ Design Considerations

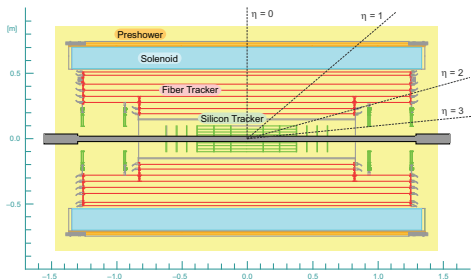


- Electromagnetic energy resolution at the level of $\delta E/E = \frac{0.05}{\sqrt{E}}$ with good $\pi^0 - \gamma$ separation
- good muon momentum resolution and muon ID
- Hadron energy resolution of about $\delta E/E = \frac{0.8}{\sqrt{E}}$:
 - ▶ p_T^{jet} , m^{jet} , and E_T are critically dependent upon it.
- Missing transverse energy resolution:
 - ▶ angular coverage down to about 1°
 - ▶ minimizing dead areas in the large angle calorimetry

Upgraded DØ

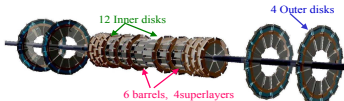
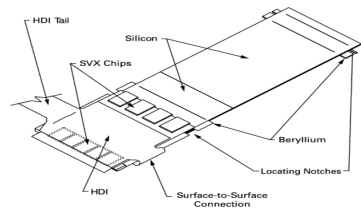


Central Tracker



- ▶ A Silicon Microstrip Tracker (SMT) and a Central Fiber Tracker (CFT) within a solenoidal magnet
- ▶ Excellent resolution; $\sigma_{d_0} \approx 15\mu m$, $\sigma_{z_0} \approx 35\mu m$:
b-tagging, good $p_T^{lep/jet}$ and E_T measurement

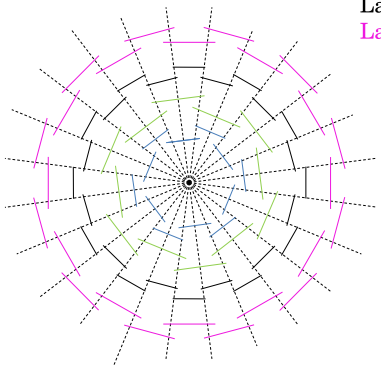
Silicon Microstrip Tracker



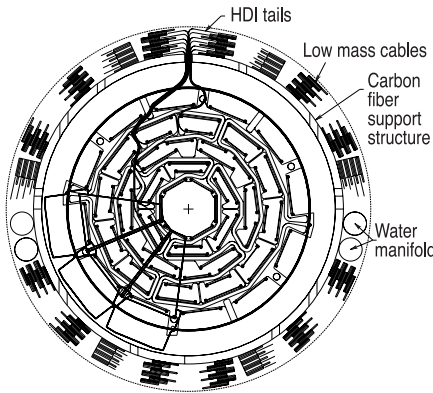
Silicon μ -strips	Barrels	Inner disks	Outer disks
Type of ladders	Single, double-sided	Double-sided	Double-sided
Stereo angle	$0^\circ, 20^\circ$ and 90°	7.5°	15°
Inner radius	2.7 cm	2.6 cm	9.5 cm
Outer radius	9.5 cm	10.5 cm	26 cm
# of channels	400K	250K	150K

- ▶ **Design considerations:**
minimal mass, precise alignment, good thermal performance and front-end electronics.
- ▶ The barrel gives (r, ϕ) coordinate and disks give (r, ϕ, z) .
- ▶ **Unit cell:**
1/2 silicon surfaces a laminated readout chip glued to rectangular beryllium substrates.

Silicon Microstrip Tracker

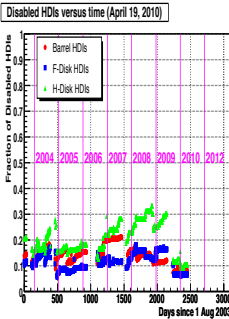
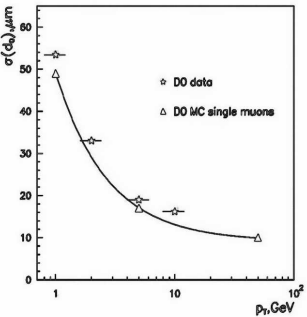
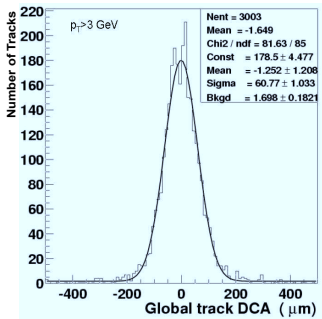


Layer 1
Layer 2
Layer 3
Layer 4



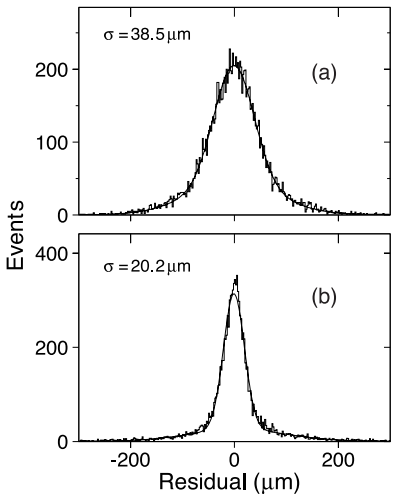
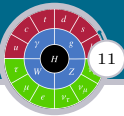
Cross section of the SMT disk/barrel module showing ladders mounted on the beryllium bulkhead, sample cable paths, three of twelve F-disk wedges, carbon fiber support structure, and the low-mass cable stack.

Silicon Microstrip Tracker Performance



- The signal/noise ratio is between 12 – 18 depending on the module type
- $\sigma_{d_0} \approx 60 \mu\text{m}$ to which the beam size itself contributes 30 to $40 \mu\text{m}$

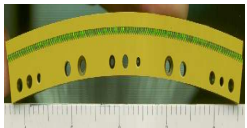
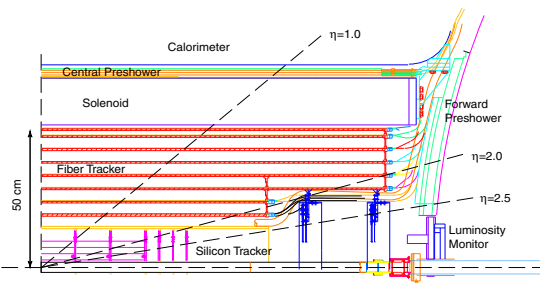
Silicon Microstrip Tracker Performance



Axial residual distribution using tracks
with $p_T > 3\text{GeV}/c$

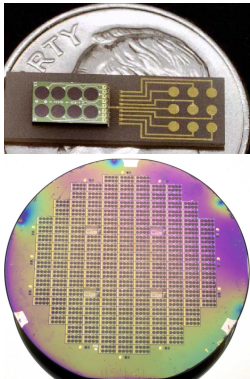
- a) upon initial installation and
- b) after software alignment of the central barrel detectors.
- ▶ the residual is the distance between the SMT hit and the track.
- ▶ the track fit was done using all SMT and CFT hits except the SMT hit in question.
- ▶ the simulated resolution of the residual distribution for a perfectly aligned detector is about 16μ .

Central Fiber Tracker



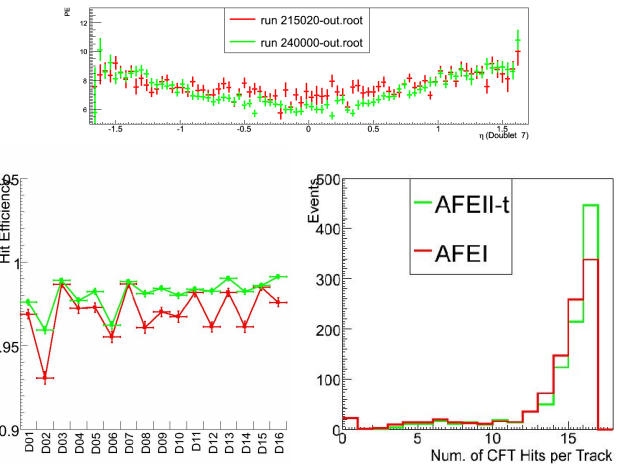
- ▶ 8 coaxial carbon cylinders, each supporting 2 doublet layers of fibers in axial-u-v orientation (3)
- ▶ 76800 fibers: made of polystyrene (PS), *paraterphenyl* (PT) 1%, and *3-hydroxyflavone* (3HF) 0.15%;
 $d = 835\mu m; l = 1.66/2.52m$

Central Fiber Tracker Light Collectors



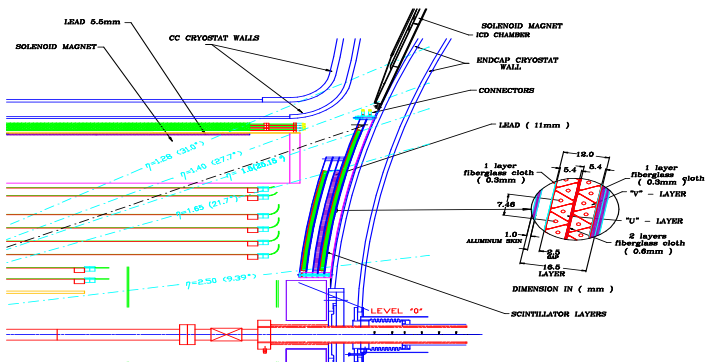
- the fibres are connected by $7 - 11m$ long optical waveguides to photodetectors positioned in a cryostat underneath the central calorimeter
- light collectors are Visible Light Photon Counters (VLPCs), (arsenic doped silicon diodes operating at temperatures of $10K$)
- the VLPCs have quantum efficiencies of $\approx 80\%$, high gain and less than 0.1% average noise
- the axial fibre layers are used in the Level 1 trigger system

Central Fiber Tracker: performance



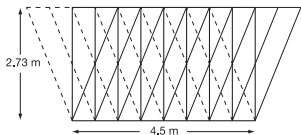
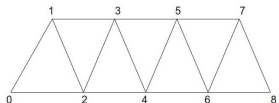
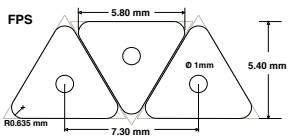
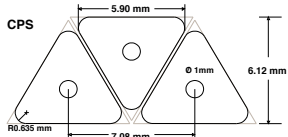
average photon yield, hit efficiency, and number of CFT hits per track

Preshower detector



- ▶ calorimetry as well as tracking detectors:
electron ID and background rejection at online triggering
and offline reconstruction.

Central Preshower Detector

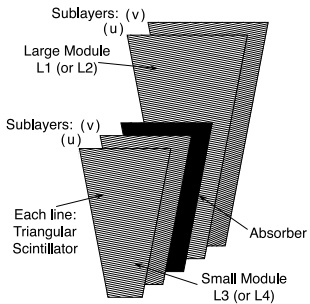


- three concentric cylindrical layers of 1280 scintillators, arranged in an axial-u-v (23°) geometry
- scintillators:
 - ▶ triangular strips with a wavelength-shifter at center of each strip and a waveguide transferring light to outer VLPCs.
 - ▶ made of extruded polystyrene (PS), *paraterphenyl* (PT) 1%, and *diphenyl stilbene* (DS) 0.15%

Forward Preshower detector

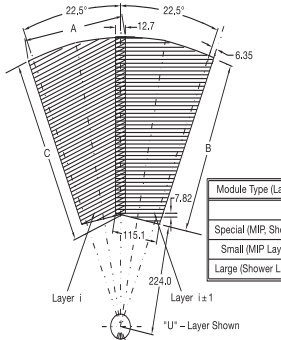
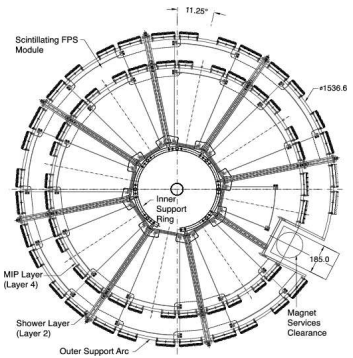


- Charged particles passing through the detector will register minimum ionizing signals in the MIP layer → tracking.
- Electrons shower in the absorber → a cluster of energy, which is then matched to MIP-layer signal.
- Photons will not generally interact in the MIP layer, but will produce a shower signal in the shower layer.
- Heavier charged particles are less likely to shower, typically producing a second MIP signal in the shower layer.



FPS module with $u - v$ MIP and shower layers, separated by a lead and stainless steel absorber.

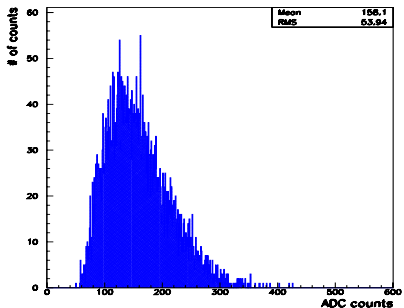
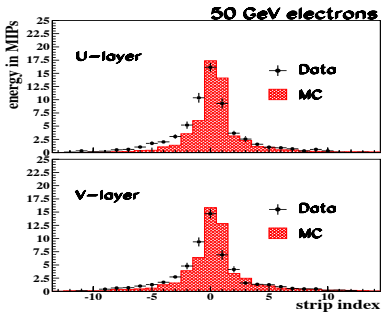
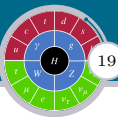
Forward Preshower Detector



Module Type (Layer)	Dimension (in mm)		
	A	B	C
Special (MIP, Shower)	214.9	250.9	278.3
Small (MIP Layer)	255.3	352.3	381.7
Large (Shower Layer)	312.6	496.6	528.7

$r - \phi$ view of the north FPS detector. For clarity, only layers 2 (shower) and 4 (MIP) are shown; layers 1 (shower) and 3 (MIP) are rotated by 22.5 degrees in ϕ with respect to these layers so their supports do not overlap.

Forward Preshower Detector

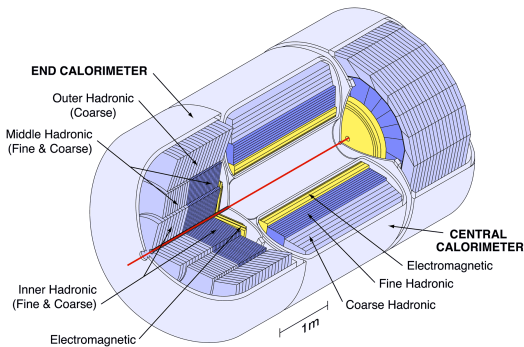


- ▶ left: the shower profile of 50GeV electrons in the FPS for both the u and the v module layers.
- ▶ right: The MIP spectrum for 125 GeV pions traversing the u layer of the forward FPS module.

Calorimeter



20



Uranium/liquid-Argon (ULA) sampling calorimetry

□ Design considerations:

1) good energy resolution and $e/\gamma/\pi$ separation → fine segmentation

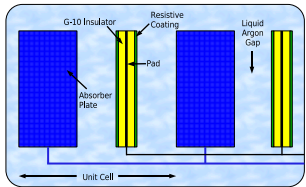
► three liquid argon cryostats(90K): one central, and two forward backward endcaps (coverage up to $\approx 2^\circ$)

Calorimeter Unit Cell



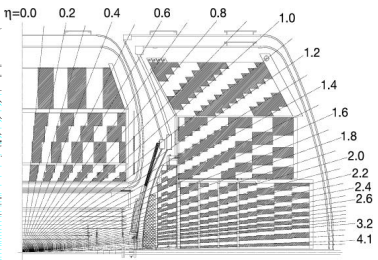
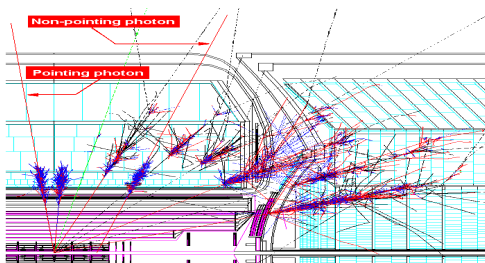
21

- an insulating layer separates the pads from the outer surface.
- several unit cells stacked on top of each other are read out together (≈ 47000 channels).
- **Uranium is a better absorber compared to Cu/Fe:**
 - 1) much better energy resolution for hadrons and jets
 - 2) the short absorption length



an absorber plate (U, Cu or Fe followed by a gap filled with liquid argon and a G – 10 board, with a $\Delta V = 2.0\text{ kV}$ at the middle

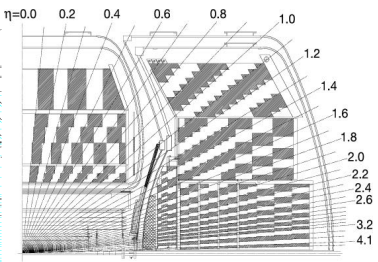
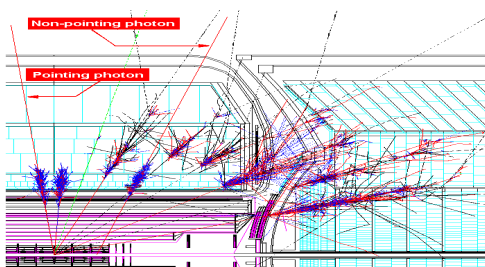
Central Calorimeter



- multi-layer EM and hadronic modules:

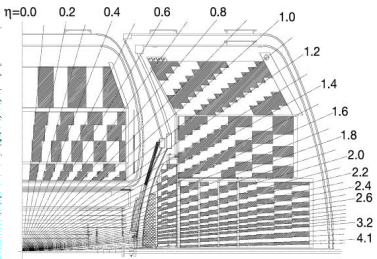
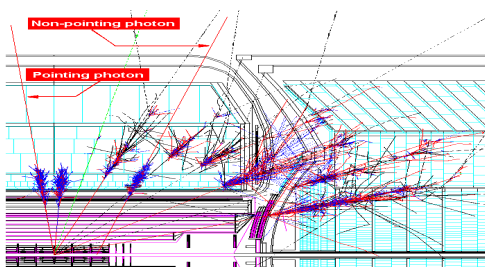
Layer	CC	EC
EM 1,2,3,4	$X_0: 2,2,7,10$ 3 mm Ur	$X_0: (0,3),3,8,9$ (1.4 mm Fe) 4 mm Ur
FH 1,2,3,(4)	$\lambda_0: 1.3,1.0,0.9$ 6 mm Ur	$\lambda_0: 1.3,1.2,1.2,1.2$ 6 mm Ur
CH 1,(2,3)	$\lambda_0: 3$ 46.5 mm Cu	$\lambda_0: 3,3,3$ 46.5 mm Fe

Central Calorimeter



- The transverse sizes of the readout cells \approx transverse sizes of showers: $1 - 2\text{cm}$ for EM showers and about 10cm for hadronic showers
Towers in both EM and hadronic modules are $\delta\eta = 0.1$ and $\delta\phi \approx 5^\circ$

Central Calorimeter



- dead region in between the three cryostats.
 - a single layer array of 384 scintillating tiles mounted on the face of both end cryostats.
 - The scintillation light is taken by optical fibres to phototubes outside the magnetic field region.

Calorimeter Calibration



► Online calibration:

- ▶ Pulse shape measurements
- ▶ Liquid argon purity
- ▶ Reflection (impedance) measurements
- ▶ Timing corrections

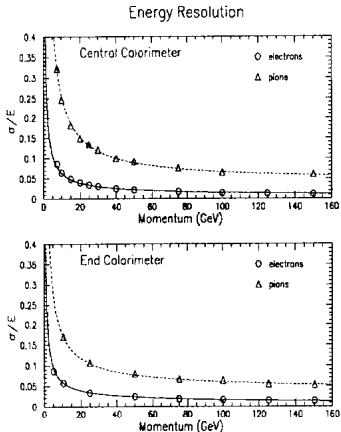
► Offline calibration:

- ▶ Data quality control
- ▶ Trigger performance
- ▶ ϕ inter-calibration
- ▶ Absolute EM scale from W/Z , J/ψ , etc.
- ▶ Electron ID, Jet ID and missing ET
- ▶ Energy flow jet algorithm
- ▶ track-calorimeter combination

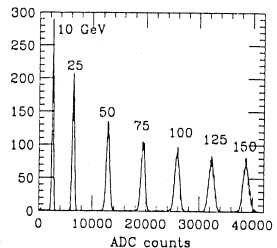
Calorimeter Performance



24

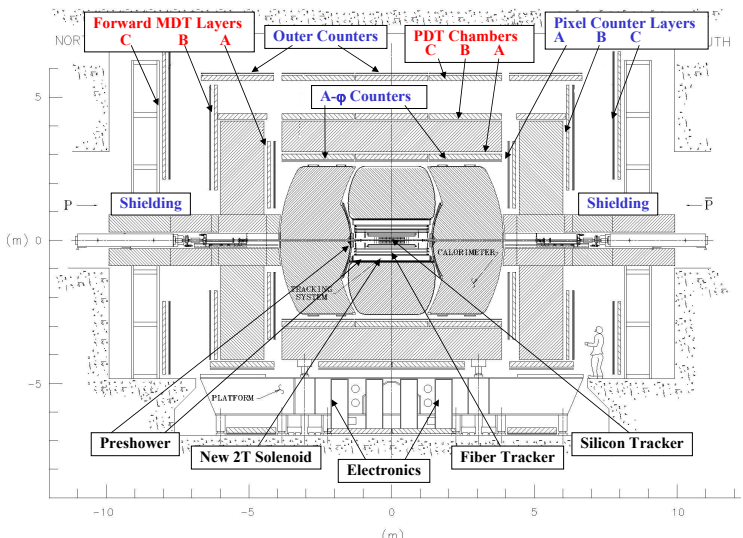


Normalized distribution



left: π and electron energy resolution; right: ADC counts for electrons

Muon Detector

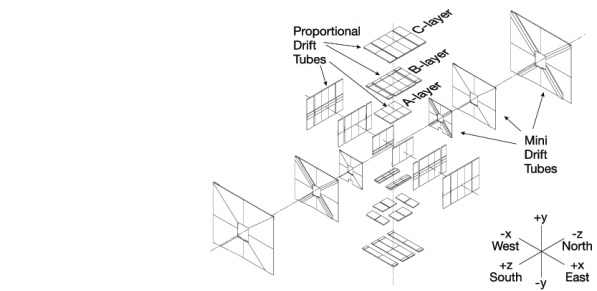


Muon Tracking System



- ▶ **Why a muon tracking system**
 - i*) enables a low-pT cutoff in the Level 1 muon trigger
 - ii*) allows for cleaner matching with central detector tracks
 - iii*) rejects π/K decays
 - iv*) improves the momentum resolution for high momentum muons.
 - ▶ **Toroidal magnet:**
 - 8/10 superconducting coils ($r = 60\text{cm}$, $l = 250\text{cm}$) carrying 1500A – current reversing switches → same amount of collected data in each polarization

Muon Tracking System



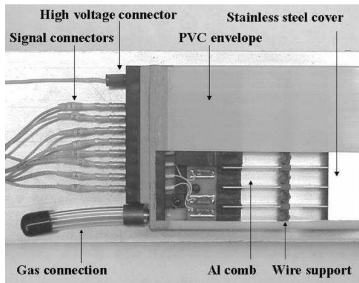
- three layers of drift chambers, located inside (A layer) and outside (B and C layers) of the central toroid
in total 94 PDT chambers with 6624 cells.
- The $2.8 \times 5.6 m^2$ chambers (3 or 4 decks of PDT), are filled with 84% Argon, 8% CF_4 , and 8% CH_4 (fast and non-flammable).

Muon Tracking System: PDT



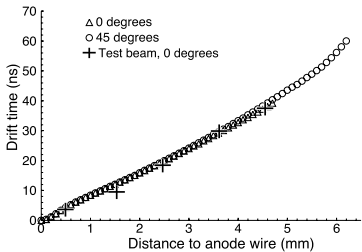
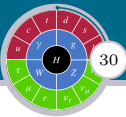
- Anodes are held at 4.7kV and electrodes at 2.3kV The maximum electron drift time in the 10cm wide drift cell is 450ns
- The cathode pads are made of thin copper-clad Glasteel
- **For each PDT hit:**
 - ▶ the electron drift time,
 - ▶ Δt , the difference in the arrival time of the signal pulse at the end of the hit cell's wire and at the end of its readout partner's wire
 - ▶ the charge deposition on the cathode is measured.
- only the A-layer pads are fully instrumented with electronics. about 10% of the B-and C-layer pads are instrumented.

Muon Forward Tracking System



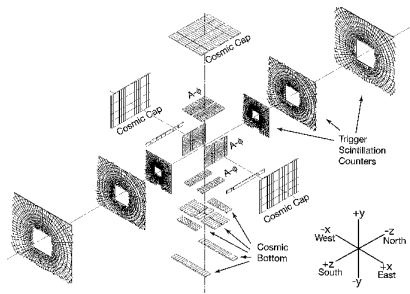
- ▶ The MDT system consists of 6080 mini drift tubes ($9.4 \times 9.4\text{mm}^2$) that are assembled into six layers of eight octants each.
- ▶ **anodes:** eight $50\mu\text{m}$ gold-plated tungsten
- ▶ **gas mixture:** 90% CF_4 and 10% CH_4 .

Muon Forward Tracking System



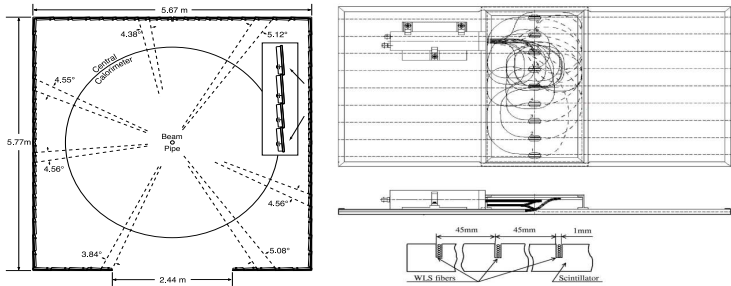
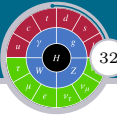
- each anode wire is connected to an amplifier discriminator board (ADB)
output logical differential signals from the ADB are sent to digitizing electronics which measure the signal arrival time with an accuracy of 18.8 ns.
- tracking efficiency $\approx 99\%$ perpendicular to the MDT plane
overall $\approx 95\%$ (due to the wall thickness and PVC sleeves)
– DØ Detector – Sina Bahrasemani – Fall 2017 –

Muon Scintillation Counters



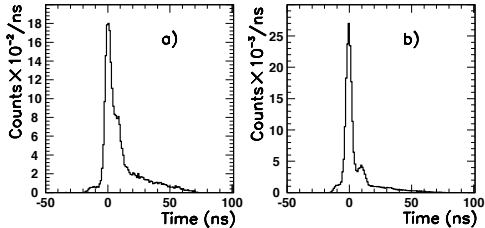
- ▶ 2/3 central/forward scintillation counters layers.
- ▶ provide a fast timing signal to associate a muon in a PDT with the appropriate bunch crossing and discriminate against the cosmic ray background.

Muon $A\phi$ Scintillation Counters



- ▶ Nine barrels of counters cover $|\eta| < 1.0$.
- ▶ $\delta\phi \approx 4.5^\circ$; $\delta\ell \approx 80\text{cm}$ to match CFT segmentation and time resolution of PDT
- ▶ $12.7 - \text{mm} - \text{thick}$ BICRON 404A scintillator with BICRON BCF 92 wavelength shifter fiber

Muon $A\phi$ Scintillation Counters Performance



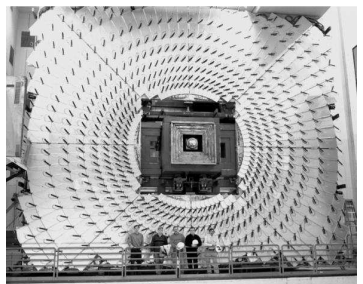
The time-of-arrival distributions recorded by $A\phi$ counters in events triggered by a) all triggers b) muon triggers only.

- ▶ the peaks around zero in both figures are from muons originating at the interaction region
- ▶ the time resolution of all 630 $A\phi$ counters combined is $\sigma_t = 2.5\text{ns}$

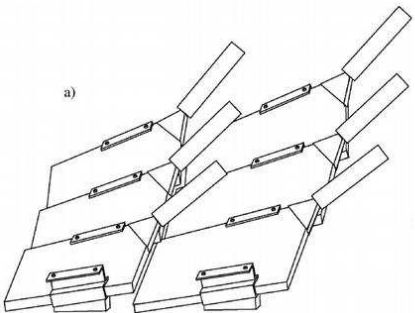
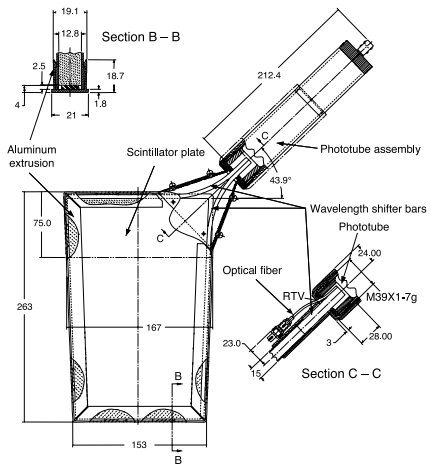
Muon Forward Scintillation Counters



- 4214 trapezoidal counters are arranged in an $r - \phi$ geometry in about twelve concentric zones in the radial direction ($1.0 < |\eta| < 2.0$)
- the segmentation:
 - i) matches the ϕ segmentation of the CFT
 - ii) the minimum muon trigger momentum threshold
 - iii) muon multiple scattering in the toroids
 - iv) background trigger rates due to accidental coincidences (combinatoric background rejection scales as N^m for m layers of N counters.)

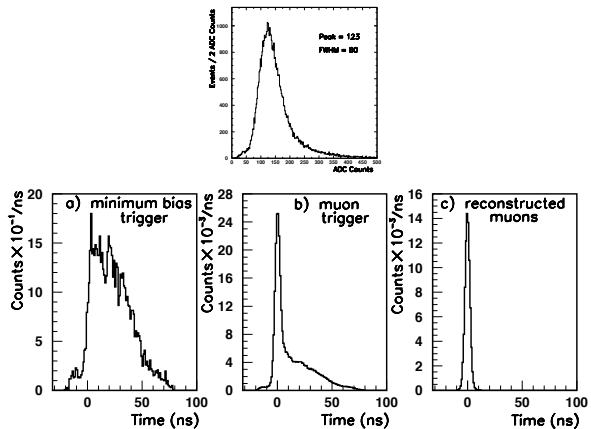


Muon Forward Scintillation Counters



Left: The design of a pixel scintillation counter. Right: counters arrangement

Muon Forward Scintillation Counters Performance

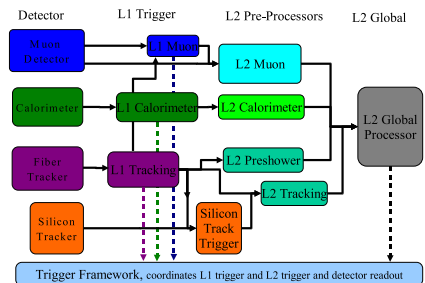


Top: Muon pulse height distribution for all 4214 pixel counters. Bottom: Time spectra of hits recorded by pixel counters: a) minimum bias trigger; b) muon trigger; c) reconstructed muons.

Trigger System



- ▶ L1 ($2.5\text{MHz} \rightarrow 1.5\text{kHz}$), the individual sub-systems are mostly independent, except for the ability to match muons to central tracks.
- ▶ L2 ($1.5\text{kHz} \rightarrow 850\text{Hz}$), sub-detector specific objects are reconstructed in separate pre-processors.
- ▶ the L2 global processor constructs physics objects.
- ▶ The L1 and L2 allow for up to 128 individual triggers
- ▶ L3 ($850 \rightarrow 20/30\text{Hz}$)





37

Thank you

DØ Experiment Goals



□ Z and W masses:

- Z mass from $Z \rightarrow e^+e^-$ using invariant mass
- W mass from $W \rightarrow l\nu_l$ using

$$m_T = \sqrt{2p_T^l E_T(1 - \cos \theta_{l,MET})}$$

- good E_T resolution is necessary for m_T

DØ Experiment Goals



□ **Z and W widths:**

- $\delta\Gamma_Z = \frac{2}{N} \sqrt{\Gamma_Z^2 + (2.35\delta m_Z)^2}$
- $\frac{\Gamma_W}{\Gamma_Z}$ within 8% → QCD radiative corrections & narrowing down m_t mass window

DØ Experiment Goals



38

- **$Z \rightarrow X\gamma; X \rightarrow l^+l^-$ searches:**
 - electronic to muonic decay ratio is needed
 - good γ (> 10 GeV) and π^0 separation is essential

DØ Experiment Goals



38

- **Forward-backward asymmetry:**
 - $b\bar{b}$ decay was of special interest due to pure measurements from other experiments
 - good muon identification at $p_T \approx 100 GeV/c$

DØ Experiment Goals



38

- ▶ **Gauge boson couplings:**
 - associated production of gauge bosons –
 - $p\bar{p} \rightarrow W\gamma X; W \rightarrow l\nu$

DØ Experiment Goals



38

► W and Z production:

- The x-dependence of W and Z production reveal the parton x-distribution in the same way as in Drell-Yan production.
- The p_T distribution of produced bosons is interesting for a study of radiative processes in QCD

DØ Experiment Goals



38

- ▶ $W/Z \rightarrow q\bar{q}$:
 - good hadron energy measurement in order to reduce the error on jet invariant mass.
 - good segmentation of calorimetry is also desired

DØ Experiment Goals



38

- ▶ $\frac{\alpha_{QCD}}{\alpha_{QED}}$:
 - single γ to single g production

DØ Design Considerations



39

- Electromagnetic energy resolution at the level of $\delta E/E = \frac{0.05}{\sqrt{E}}$ with good $\pi^0 - e$ separation
 - ▶ good electron ID for narrow massive states searches and to lower electron-jet faking rate.
 - ▶ good lateral and longitudinal sampling for single γ searches with high p_T (**challenging $\pi^0 - e$ separation**)
- good muon momentum resolution and muon ID
 - ▶ muons are less analyzed, but with charge tagging \rightarrow ID them even inside jets which is important for many searches

Upgraded DØ



- in 2001 after the Main Injector and associated Tevatron upgrades the instantaneous luminosity increased by more than a factor of ten
- The central tracking system was completely replaced.
 - ▶ the old system lacked a magnetic field and suffered from radiation damage
 - ▶ improved tracking technologies are now available.
 - ▶ The new system included a silicon microstrip tracker and a scintillating-fiber tracker located within a 2 T solenoidal magnet.

Upgraded DØ

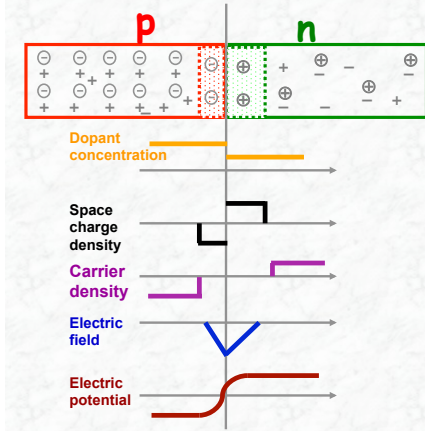


- Between the solenoidal magnet and the central calorimeter and in front of the forward calorimeters, preshower detectors have been added for improved electron identification.
- In the forward muon system, proportional drift chambers are replaced by mini drift tubes and trigger scintillation counters
 - ▶ which can withstand the harsh radiation environment and additional shielding has been added.
 - ▶ In the central region, scintillation counters have been added for improved muon triggering.

p-n Junction

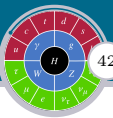


p-n-Junction



- Diffusion of e^- from n-side and h^+ from p-side
- Recombination on other side, free charges disappear around junction ("depletion")
- Neutral p- or n-Si becomes charged → E-Field
- External field can increase or decrease depletion zone
- Depletion is what we want for detectors!

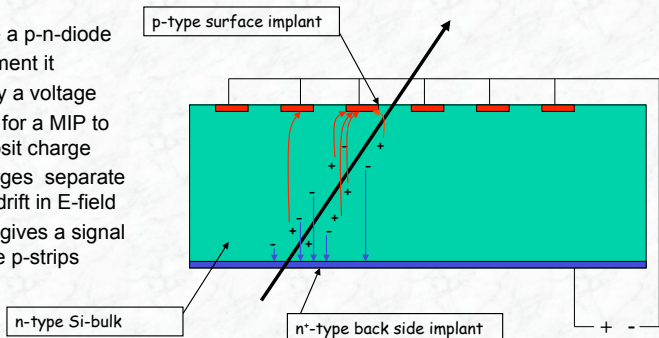
Basic Silicon Detector



42

A Basic Silicon Detector

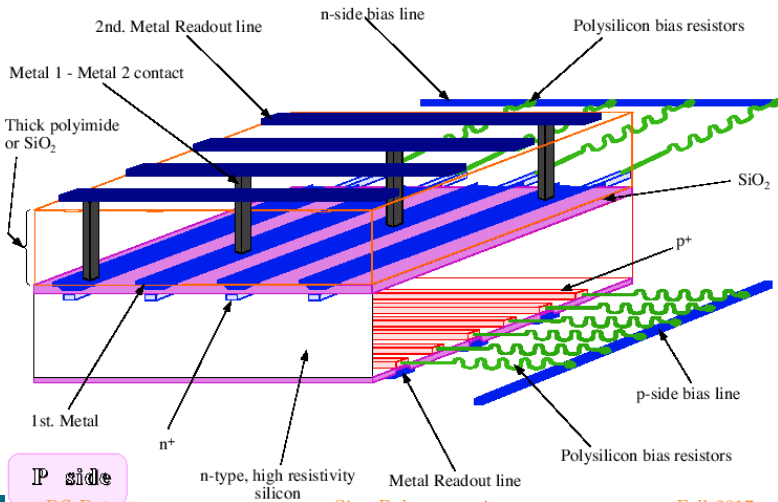
- Take a p-n-diode
- Segment it
- Apply a voltage
- Wait for a MIP to deposit charge
- Charges separate and drift in E-field
- This gives a signal in the p-strips



DSDM Silicon Detector



N side

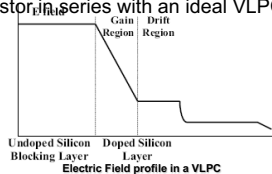
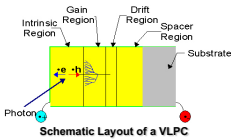


Visible Light Photon Counters



44

- The operation principle of VLPCs is the effect of impurity band.
 - Occurs when a semiconductor is heavily doped with shallow donors or acceptors.
 - The impurity atoms are close together → electrical transport occurring by charge hopping from impurity site to impurity site!
- The standard 1.12 eV gap of Si is used to absorb photons
- The small gap with the impurity band is used for creating an electron – D+ avalanche multiplication.
 - Small gap O(0.05eV) → Relatively low field is required for avalanche the required field for producing an avalanche is low.
 - Localized and self-limiting avalanche(due to local field collapse, D+ have low mobility)
- The drift region can be seen as an internal resistor in series with an ideal VLPC



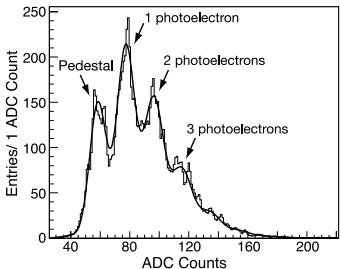
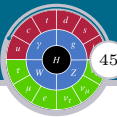
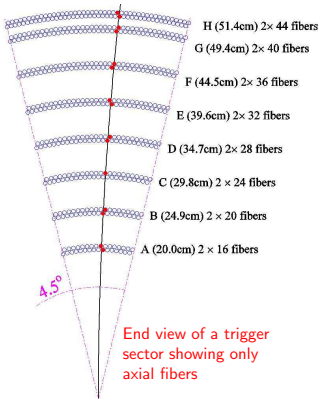


Fig. 19. A typical LED spectrum for a single VLPC for an axial CFT fiber. Every channel is fit automatically and the parameters of the fit are extracted and used for monitoring. Typically, more than 97% of the axial channels are fit successfully. The solid histogram is the data; the smooth curve is the fit.

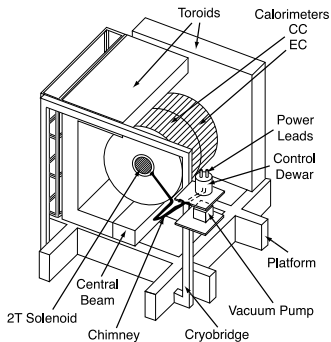
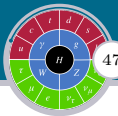
Central Track Trigger



- ▶ Counts track candidates identified in axial view of CFT by looking for hits in all 8 axial layers
- ▶ Combines tracking and preshower information to identify electron and photon candidates
- ▶ Generates track lists allowing other trigger systems to perform track matching

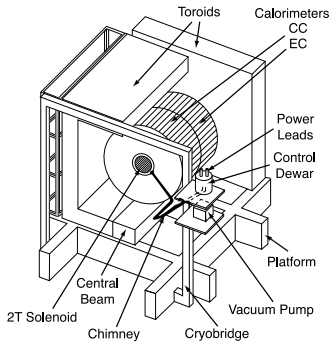


Solenoidal Magnet



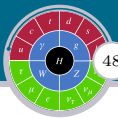
- to optimize the momentum resolution, $\delta p_T / p_T$ and tracking pattern recognition → a central field of 2T
- design criteria:
 - i) to operate safely and stably at either polarity
 - ii) a uniform field over as large a percentage of the volume as practical,
 - iii) as thin as possible to make the tracking volume as large as possible,
 - iv) an overall thickness of approximately $1X_0$ at $\eta = 0$ to optimize the performance of the central preshower detector mounted on the outside of the solenoid cryostat.

Solenoidal Magnet



- to optimize the momentum resolution, $\delta p_T / p_T$ and tracking pattern recognition → a central field of 2T
- design criteria:
 - i) to operate safely and stably at either polarity
 - ii) a uniform field over as large a percentage of the volume as practical,
 - iii) as thin as possible to make the tracking volume as large as possible,
 - iv) an overall thickness of approximately $1X_0$ at $\eta = 0$ to optimize the performance of the central preshower detector mounted on the outside of the solenoid cryostat.

Solenoidal Magnet



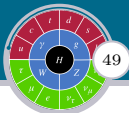
48

Major parameters of the solenoid

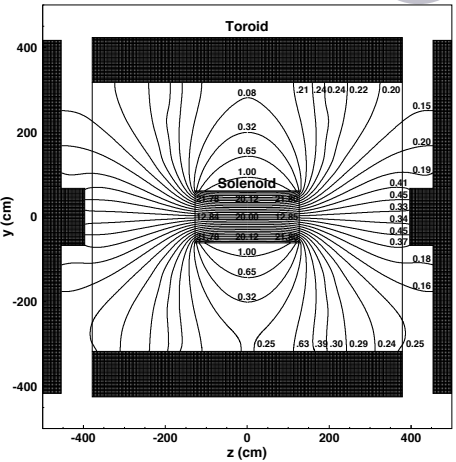
Central field	2.0 T
Operating current	4749 A
Cryostat warm bore diameter	1.067 m
Cryostat length	2.729 m
Stored energy	5.3 MJ
Inductance	0.47 H
Cooling	Indirect, 2-phase forced flow helium
Cold mass	1460 kg
Conductor	18-strand Cu:NbTi, cabled
Conductor stabilizer	High purity aluminum
Thickness	0.87 X ₀
Cooldown time	≤ 40 hours
Magnet charging time	15 minutes
Fast discharge time constant	11 seconds
Slow discharge time constant	310 seconds
Total operating heat load	15 W plus 0.8 g/s liquefaction
Operating helium mass flow	1.5 g/s

The solenoid is wound with two layers of superconductor to achieve the required linear current density for a 2T central field.

Magnet Field



- ▶ Within the solenoid (operated at $4749A$), The calculated magnetic field is scaled by 0.09% to agree with the measurement.
 - ▶ Within the toroid (operated at $1500A$) The calculated magnetic field is scaled by 4.3%

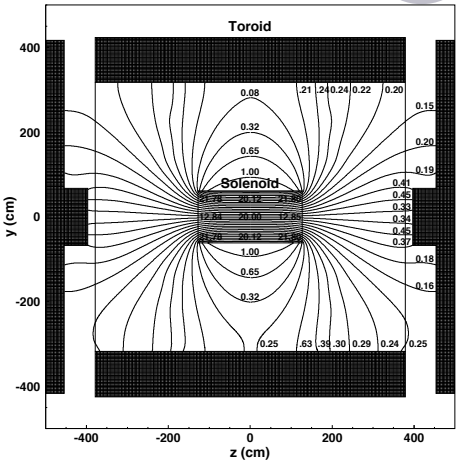


The $y - z$ view of the $D\emptyset$ magnetic field (in kG).
The field in the central toroid is approximately
 $1.8T$

Magnet Field



- ▶ Within the solenoid (operated at 4749A), The calculated magnetic field is scaled by 0.09% to agree with the measurement.
- ▶ Within the toroid (operated at 1500A) The calculated magnetic field is scaled by 4.3%



The $y - z$ view of the $D\bar{\Omega}$ magnetic field (in kG).
The field in the central toroid is approximately

$$1.8T$$

CALO Readouts

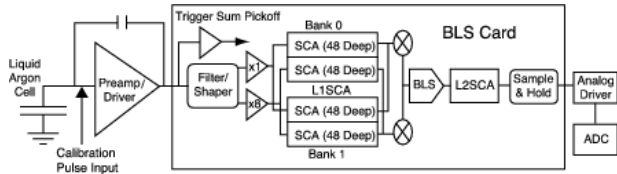
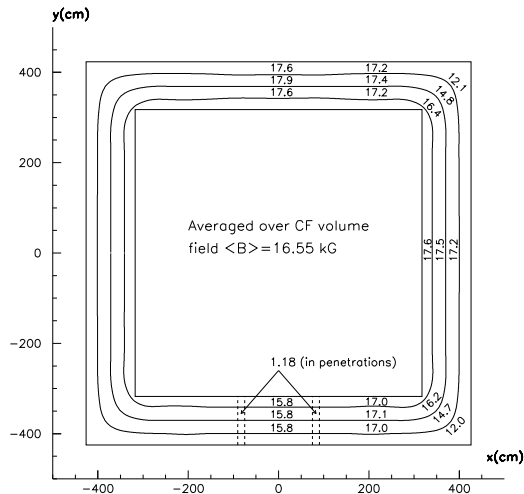


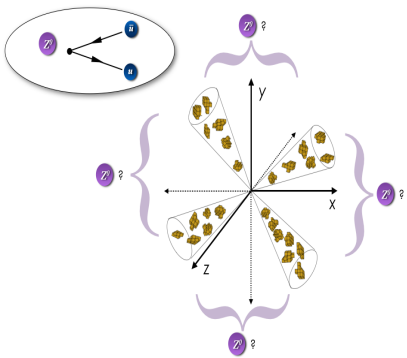
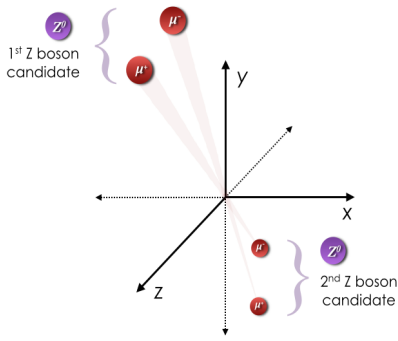
Fig. 34. Readout chain of the calorimeter in Run II indicating the three major components: preamplifiers, baseline subtractor and storage circuitry (BLS), and the ADCs.

Muon Tracking System



Magnetic field in the central toroid magnet. The magnetic field is in $k\text{G}$.

Combinatorial Background



- ▶ the non-background background!

Differential Signaling

